



LRRC8 channel activation and reduction in cytosolic chloride concentration during early differentiation of C2C12 myoblasts

Lingye Chen^a, Benjamin König^a, Tobias Stauber^{a, b, *}

^a Institute of Chemistry and Biochemistry, Freie Universität Berlin, Thielallee 63, 14195, Berlin, Germany

^b Department of Human Medicine and Institute for Molecular Medicine, MSH Medical School Hamburg, Am Kaiserkaai 1, 20457, Hamburg, Germany

ARTICLE INFO

Article history:

Received 11 August 2020

Accepted 23 August 2020

Available online 4 September 2020

Keywords:

C2C12 myoblasts

Chloride channel

Intracellular chloride

Myogenesis

Volume-regulated anion channel

ABSTRACT

Leucine-rich repeat containing family 8 (LRRC8) proteins form the volume-regulated anion channel (VRAC). Recently, they were shown to be required for normal differentiation and fusion of C2C12 myoblasts, by promoting membrane hyperpolarization and intracellular Ca^{2+} signals. However, the mechanism by which they are involved remained obscure. Here, using a FRET-based sensor for VRAC activity, we show temporary activation of VRAC within the first 2 h of myogenic differentiation. During this period, we also observed a significant decrease in the intracellular Cl^- concentration that was abolished by the VRAC inhibitor carbenoxolone. However, lowering the intracellular Cl^- concentration by extracellular Cl^- depletion did not promote differentiation as judged by the percentage of myogenin-positive nuclei or total myogenin levels in C2C12 cells. Instead, it inhibited myosin expression and myotube formation. Together, these data suggest that VRAC is activated and mediates Cl^- efflux early on during myogenic differentiation, and a moderate intracellular Cl^- concentration is necessary for myoblast fusion.

© 2020 The Authors. Published by Elsevier Inc. This is an open access article under the CC BY license (<http://creativecommons.org/licenses/by/4.0/>).

1. Introduction

Myoblast differentiation and fusion, critical processes in skeletal muscle development and regeneration, are coordinated by a complex network of proteins and signaling molecules [1–3]. This includes a tightly regulated transmembrane movement of the cations K^+ and Ca^{2+} [4–8]. The action of potassium channels leads to the hyperpolarization of the differentiating cell [9–11], facilitating the activation of voltage-gated Ca^{2+} channels [4,12]. Preventing membrane hyperpolarization inhibits the expression of the myogenic transcription factors myogenin and myocyte enhancer factor-2 [5,7]. An increase in the intracellular Ca^{2+} concentration ($[\text{Ca}^{2+}]_i$), due to Ca^{2+} influx from the extracellular space [4,6,13] or transient Ca^{2+} release from the endoplasmic reticulum [6,8], is essential for myoblast differentiation. Decreased extracellular or intracellular

Abbreviations: CBX, carbenoxolone; FRET, fluorescence resonance energy transfer; LRRC8, leucine-rich repeat containing family 8; SPQ, 6-methoxy-*N*-(3-sulfopropyl)quinolinium; VRAC, volume-regulated anion channel.

* Corresponding author. Department of Human Medicine and Institute for Molecular Medicine, MSH Medical School Hamburg, Am Kaiserkaai 1, 20457, Hamburg, Germany.

E-mail address: tobias.stauber@medicalschooll-hamburg.de (T. Stauber).

<https://doi.org/10.1016/j.bbrc.2020.08.080>

0006-291X/© 2020 The Authors. Published by Elsevier Inc. This is an open access article under the CC BY license (<http://creativecommons.org/licenses/by/4.0/>).

Ca^{2+} concentrations inhibit myotube formation [6,13], whereas raised $[\text{Ca}^{2+}]_i$ significantly accelerates myoblast fusion [12]. Whilst the functions of K^+ and Ca^{2+} during skeletal myogenesis have been studied extensively, little is known about the role of the anion Cl^- in this process.

The volume-regulated anion channel (VRAC) has been shown to be involved in murine myoblast differentiation [14], which was recently confirmed by an independent study [15] and which may contribute to the thinned skeletal muscle in mice lacking the essential VRAC subunit LRRC8A [16]. VRAC is a plasma membrane channel formed by LRRC8 hetero-hexamers formed by the obligatory LRRC8A and at least one of the other four LRRC8 family members (LRRC8B-E) [17,18], all of which are expressed in myoblasts [19]. It is activated upon osmotic cell swelling or under isovolumetric conditions through various signaling pathways and mediates the flux of Cl^- and organic osmolytes [20,21]. Inhibition of VRAC impairs the hyperpolarization of myoblasts and consequently prevents the sustained increase in $[\text{Ca}^{2+}]_i$ [14]. Pharmacological data suggest that VRAC, which is expressed and can be activated in proliferating C2C12 cells [19,22,23], plays an important role only within the first 6 h after induction of differentiation [14]. However, the mechanism by which VRAC contributes to myogenesis has not been fully resolved. Pharmacological inhibition of VRAC and

suppression of VRAC currents by overexpression of LRRC8A [17,18] argue for a role of VRAC channel activity [14], but direct evidence for a transient VRAC activation at the onset of myoblast differentiation is lacking. Furthermore, it is unclear whether there is a flux of Cl^- through VRAC and how changes in $[\text{Cl}^-]_i$ affect myoblast differentiation and fusion.

In the present study, we monitor transient VRAC activation during early myoblast differentiation using a fluorescence resonance energy transfer (FRET)-based sensor [24]. We show for the first time that C2C12 myoblast differentiation is accompanied by a significant decrease in cytosolic Cl^- . We find that Cl^- depletion does not affect myoblast differentiation but inhibits fusion.

2. Materials and methods

2.1. Cell culture

HeLa cells (Leibniz Forschungsinstitut DSMZ, Germany) and C2C12 mouse skeletal muscle myoblasts (ATCC, USA) were cultured in growth medium (DMEM supplemented with 10% fetal bovine serum, 100 units/ml penicillin and 100 $\mu\text{g}/\text{ml}$ streptomycin) at 37 °C in 5% CO_2 . Confluent C2C12 cells were induced to undergo myogenic differentiation by reducing the serum concentration to 2% horse serum. In chloride-reduced DMEM (PAN-Biotech, Germany), KCl and NaCl, which account for 99.5% of the total chloride content in DMEM, were replaced by potassium gluconate and sodium gluconate.

2.2. Cell transfection

Expression plasmids for human LRRC8A-Cerulean (LRRC8A with mCerulean3 fused to its C-terminus) and LRRC8E-Venus were described previously [24]. For co-expression, constructs were co-transfected into cells plated in 35 mm glass bottom dishes (Mat-Tek, USA) using FuGENE 6 (Promega, USA) according to the manufacturer's instructions. 500 ng and 2 μg of each plasmid DNA were used on HeLa and C2C12 cells, respectively. Cells were used for FRET experiments 1 day after transfection.

2.3. Sensitized-emission FRET (seFRET) measurements

FRET experiments were in principle performed as previously described [24]. 50–70% confluent C2C12 cells were used in experiments with changes in tonicity. Isotonic (340 mOsm) imaging buffer contained (in mM): 150 NaCl, 6 KCl, 1 MgCl_2 , 1.5 CaCl_2 , 10 glucose, 10 HEPES, pH 7.4. Hypotonic (250 mOsm) buffer had a decreased NaCl concentration of 105 mM. 80–100% confluent C2C12 cells were used to measure FRET changes during myogenic differentiation in isotonic differentiation buffer (329 mOsm, containing in mM: 144 NaCl, 5 KCl, 2 CaCl_2 , 1 MgCl_2 , 10 glucose, 10 HEPES, pH 7.4). 80–100% confluent HeLa cells were used as control. All FRET experiments were performed at room temperature on a Dmi6000B microscope (Leica Microsystems, Germany) equipped with a 63 \times /1.4 objective and a DFC360 FX camera. Samples were excited with EL6000 light source; emission was recorded with high speed external Leica filter wheels with Leica FRET set filters (11522073). seFRET images were acquired with the same settings for donor, acceptor and FRET channels (8 \times 8 binning, 100 ms exposure, gain 1) every 10 s (for buffer change experiments) or 1 min (for differentiation experiments) with the LAS AF software. Corrected FRET (cFRET) values were calculated according to:

$$cFRET = \frac{B - A \times \beta - C \times \gamma}{C}$$

where A, B and C correspond to the emission intensities of the donor, FRET and acceptor channels, respectively; β and γ are the correction factors (β = bleed-through of donor emission; γ = cross excitation of acceptor by donor excitation) generated by acceptor- and donor-only references.

2.4. Measurement of intracellular Cl^-

Intracellular Cl^- concentration ($[\text{Cl}^-]_i$) measurements using the fluorescent indicator 6-methoxy-*N*-(3-sulfopropyl)quinolinium (SPQ; Invitrogen, USA) were performed as previously described [25]. C2C12 myoblasts growing in 8-well chambers (Sarstedt, USA) were washed once with Hank's balanced salt solution (HBSS) and then incubated at 37 °C in a hypotonic solution (HBSS:H₂O = 1:1) with 5 mM SPQ for 15 min. After that, cells were incubated in HBSS for 15 min to allow recovery from the hypotonic shock. For cells cultured in Cl^- -reduced medium, an isotonic buffer with 0 mM Cl^- was used (gluconate was used as a substitute for Cl^-). Measurements were performed at room temperature on a Dmi8 microscope (Leica Microsystems) equipped with a 63 \times /1.40 NA oil-immersion objective and an OcraFlash 4.0 camera (Hamamatsu, Japan). SPQ fluorescence images were recorded at 16-bit, 4 \times 4 binning and 100 ms exposure with a DAPI filter set (Ex: 360/40, Dc: 400, Em: 425 lp). Calibration for each experiment was achieved using 4 μM nigericin (Sigma-Aldrich, USA) and 5 μM tributyltin (Sigma-Aldrich) to equilibrate intracellular and extracellular Cl^- concentrations ranging from 0 to 100 mM Cl^- in individual wells of 8-well chambers. To set the Cl^- concentrations in the calibration solution, equal molar KNO_3 substituted KCl in the original solution (in mM): 150 KCl, 2 CaCl_2 , 10 glucose, 10 HEPES, pH 7.2. Ionophores nigericin and tributyltin were added freshly, and carbenoxolone (CBX; Sigma-Aldrich) was included for calibration of CBX-treated samples. The relationship between fluorescence of SPQ and Cl^- concentration is described by the Stern-Volmer equation:

$$(F_0 / F) - 1 = K_{sv}[Q]$$

where F_0 is the fluorescence intensity without Cl^- , F is the fluorescence intensity in the presence of various concentrations of Cl^- , [Q] is the concentration of Cl^- and K_{sv} is the Stern-Volmer constant.

2.5. Immunofluorescence staining

Immunostaining was performed as described previously [14]. A mouse monoclonal anti-myogenin antibody (clone F5D, 1 $\mu\text{g}/\text{ml}$; Developmental Studies Hybridoma Bank, USA) was used.

2.6. Western blotting

For Western blot analysis, C2C12 cells were lysed in RIPA buffer containing protease inhibitor cocktails (Roche, Switzerland). 20 μg protein per lane were separated by 10% SDS-PAGE, transferred onto nitrocellulose membranes (Macherey-Nagel, Germany) and incubated with antibodies after blocking in 5% skim milk in TBS-tween. Following primary antibodies were used: mouse anti-myosin (clone MF20, 0.28 $\mu\text{g}/\text{ml}$; Developmental Studies Hybridoma Bank), mouse anti-myogenin (clone F5D, 1 $\mu\text{g}/\text{ml}$; Developmental Studies Hybridoma Bank) and rabbit anti-GAPDH (14C10, 1:2500; Cell Signaling Technology, USA). Immunoreactive signals were detected by chemiluminescence (HRP juice; PJK GmbH, Germany) with a ChemiSmart5000 digital imaging system (Vilber-Lourmat,

France). Densitometric quantification was performed with the Fiji software [26].

2.7. Image processing and quantitative analysis

Both seFRET and SPQ fluorescence images were processed with Fiji. cFRET maps were generated using PixFRET plugin [27] (threshold set to 1, Gaussian blur to 2) with a self-written macro to process movies and were measured by manually drawn regions of interest (ROIs). As absolute FRET values varied between individual cells, cFRET values of individual cells were normalized to their mean cFRET in isotonic buffer (for buffer change experiments) or their mean cFRET of recorded first 10 min (for differentiation experiments). For SPQ fluorescence images, the mean fluorescence intensity of ROIs was measured with Fiji and the mean fluorescence intensity of background was subtracted. Images of five random fields were analyzed for each sample per experiment.

2.8. Statistical analysis

All data are presented as mean \pm S.D.; p values between two groups were determined by a two-tailed Student's t -test. Significance was defined with $p < 0.05$.

3. Results

3.1. VRAC activation early during C2C12 myoblast differentiation

It was previously shown that pharmacological VRAC inhibitors impaired myoblast differentiation only when applied already during the first hours of differentiation, suggesting that VRAC activity is required early during this process [14]. Therefore, we aimed at monitoring channel activity in C2C12 myoblasts by using a non-invasive FRET sensor [24]. The proximity of the cytosolic C-terminal domains of LRRC8 subunits within the pore-forming hexamers [28–30] allows for intra-complex FRET between fluorescent proteins fused to their C-termini; and a drop in FRET efficiency mirrors the rearrangement of the C-terminal domains during VRAC activation [24]. We firstly coexpressed LRRC8A tagged with mCerulean3 (FRET donor) and LRRC8E tagged with Venus (FRET acceptor) in C2C12 cells and observed FRET during hypotonic stimulation (changing from extracellular 340 mOsm to 250 mOsm). As expected, the corrected FRET (cFRET) value robustly decreased by $\sim 10\%$ within 60 s (Fig. 1A), indicating the activation of LRRC8A-Cerulean/LRRC8E-Venus-containing VRAC complexes by osmotic swelling in C2C12 cells. We next tested for iso-osmotic VRAC activation at the onset of C2C12 myoblast differentiation. Whereas in undifferentiable HeLa cells, cFRET of LRRC8A-Cerulean/LRRC8E-

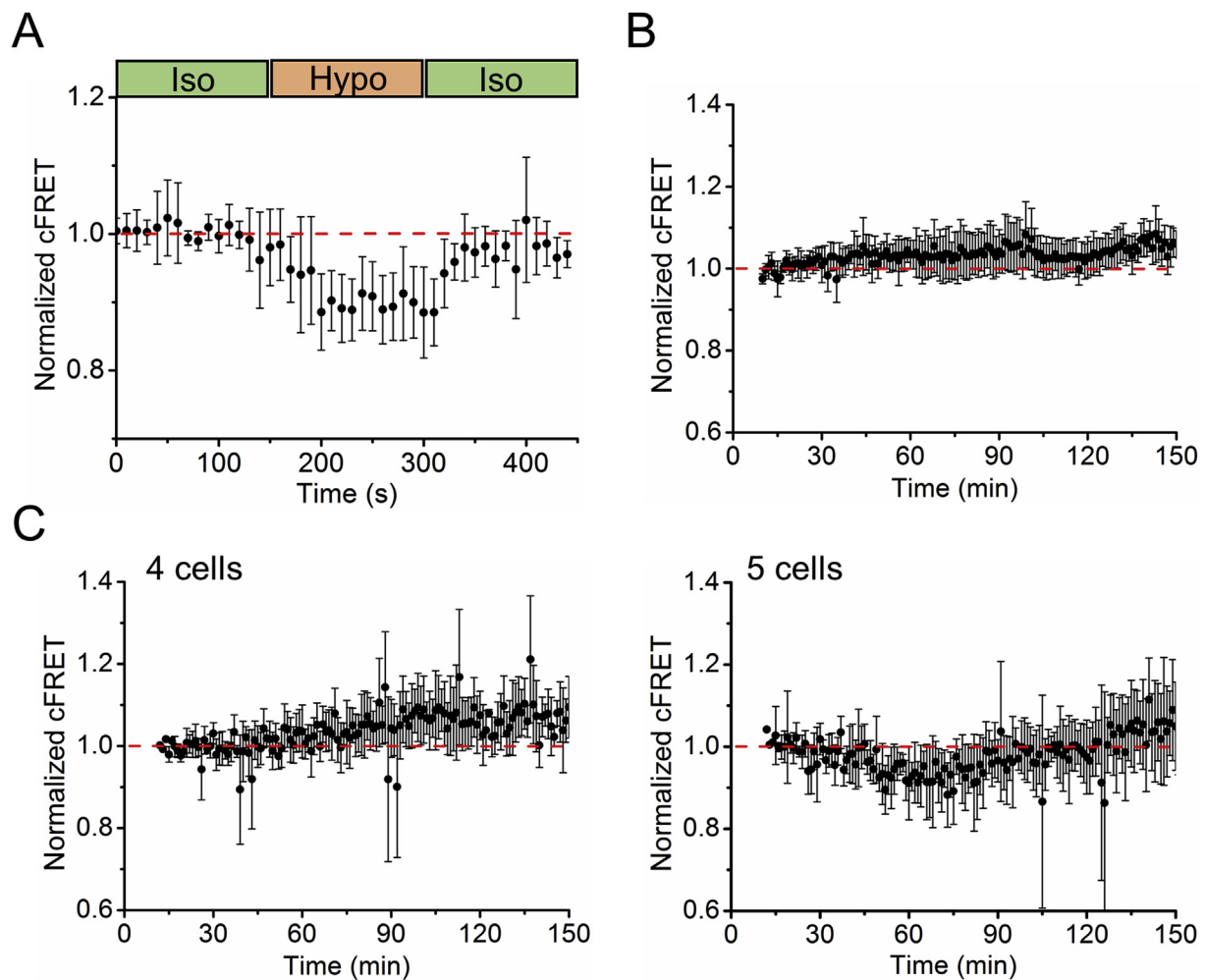


Fig. 1. VRAC activation at the onset of myoblast differentiation. A, normalized cFRET values during buffer exchange experiments with 50–70% confluent C2C12 cells ($n = 3$ dishes with 13 cells). Iso, isotonic; Hypo, hypotonic. B, normalized cFRET values during incubation of 80–100% confluent HeLa cells in isotonic differentiation buffer ($n = 5$, 14 cells). C, normalized cFRET values during incubation of 80–100% confluent C2C12 cells in isotonic differentiation buffer ($n = 7$, 9 cells). All data are presented as mean \pm S.D.

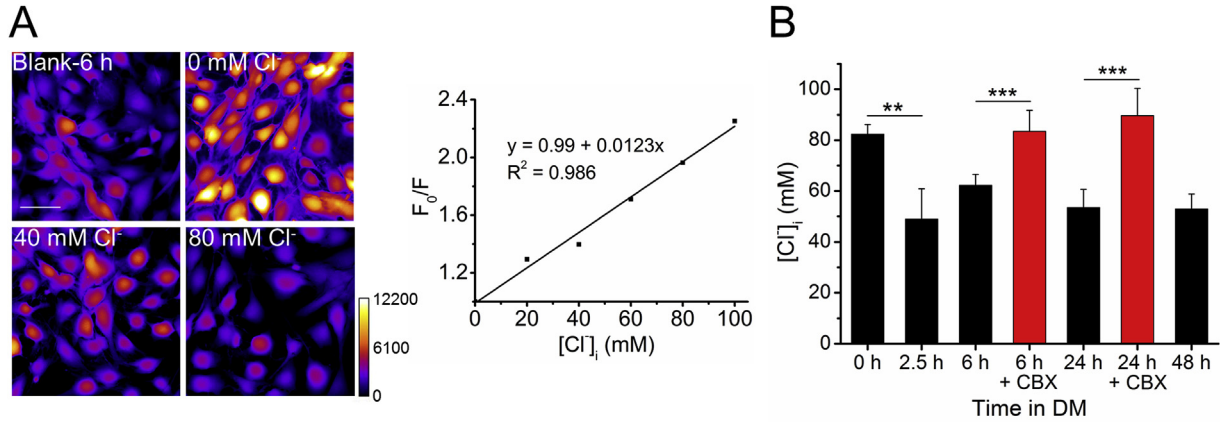


Fig. 2. Myoblast differentiation results in a [Cl⁻]_i decrease. A, representative calibration for measuring the resting [Cl⁻]_i with the fluorescence probe SPQ. Left, images of C2C12 cells stained with SPQ after 6 h of differentiation. Nigericin and tributyltin were used to equilibrate intracellular and external Cl⁻ concentrations. Fluorescence intensities are represented in color code, as shown in the calibration bar. Scale bar, 50 μm. Right, Stern-Volmer plot for the fluorescence of SPQ against Cl⁻ concentration. The resulting best linear regression fit was used to calculate the [Cl⁻]_i in (B). B, average [Cl⁻]_i of C2C12 myoblasts measured at different time points after induction of differentiation in the presence or absence of 100 μM CBX. DM, differentiation medium. Data are presented as mean ± S.D. from three independent experiments. **, *p* < 0.01; ***, *p* < 0.001 compared with the respective controls using a two-tailed unpaired *t*-test. (For interpretation of the references to color in this figure legend, the reader is referred to the Web version of this article.)

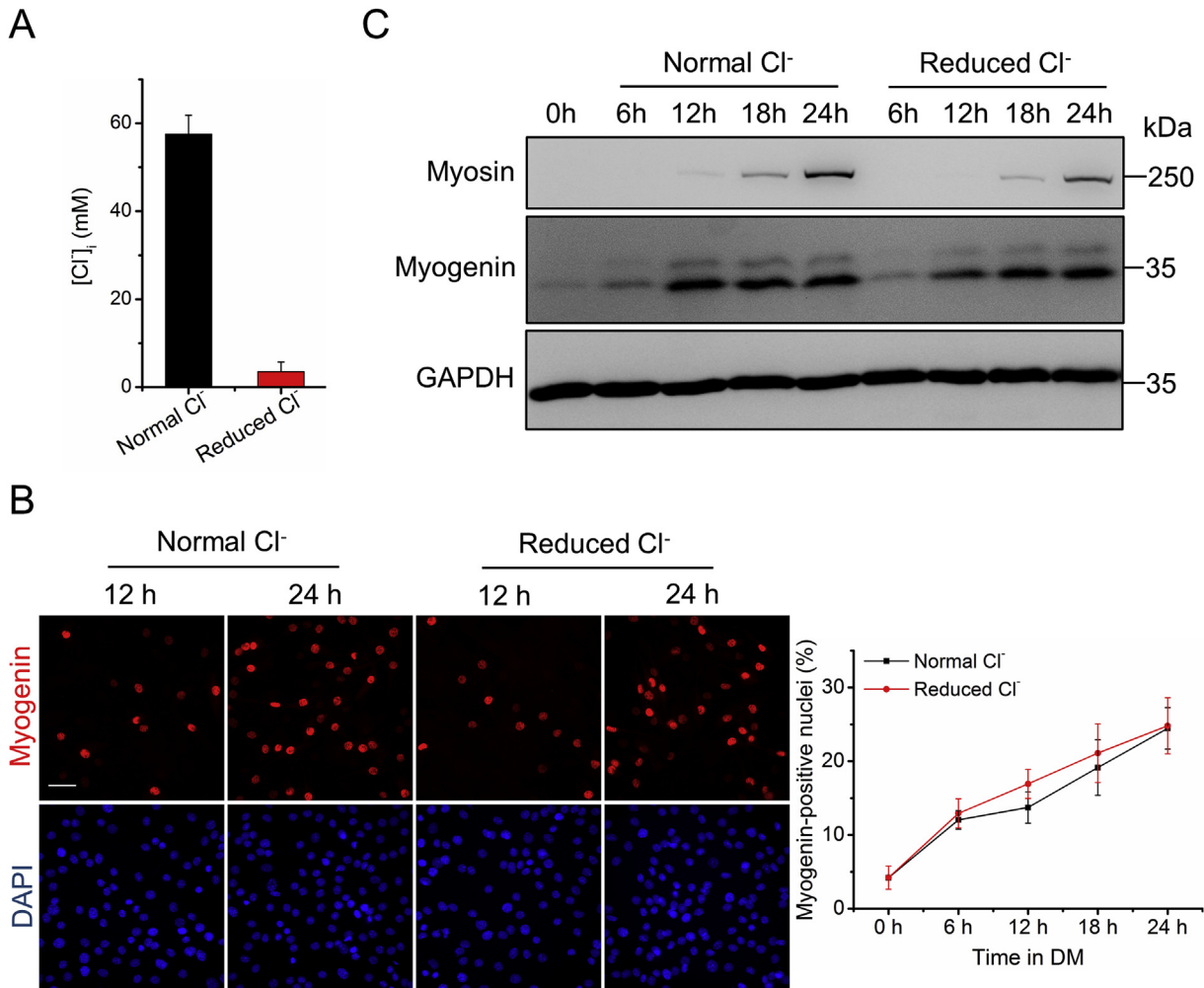


Fig. 3. Reduced extracellular Cl⁻ does not affect myoblast differentiation. A, resting [Cl⁻]_i of C2C12 cells measured after 6 h of differentiation in normal medium or Cl⁻-reduced medium. B, C2C12 myoblasts were stained with an anti-myogenin antibody (red) and DAPI (nuclei, blue) at the indicated time of differentiation. DM, differentiation medium. Scale bar, 50 μm. C, Immunoblot analysis of myogenin and myosin at the indicated time of differentiation. All data are presented as mean ± S.D. from three independent experiments. (For interpretation of the references to color in this figure legend, the reader is referred to the Web version of this article.)

Venus did not change within 2.5 h in isotonic differentiation buffer (Fig. 1B), a steady decline by ~10% occurred within the first hour of differentiation among 5 out of 9 tested C2C12 myoblasts (Fig. 1C). The presence of two populations with or without cFRET decrease (cFRET at 55–64 min differed with $p = 0.032$) is in agreement with the ratio of C2C12 cells typically undergoing differentiation. The observed cFRET decrease began at ~40 min after induction of differentiation and returned to baseline at ~120 min. These results demonstrate that VRAC is indeed activated upon induction of myoblast differentiation and its inactivation after 2 h is consistent with a role for VRAC only early in differentiation [14].

3.2. Myoblast differentiation is accompanied by an intracellular chloride decrease that is sensitive to VRAC inhibition

Depending on the LRRC8 subunits heteromerizing with LRRC8A, VRAC conducts various organic osmolytes [31–33], but all combinations mediate Cl^- conductance [21]. Therefore, we tested whether VRAC activation during myoblast differentiation leads to intracellular Cl^- changes, using the chloride indicator SPQ [25] in a calibrated, quantitative manner (Fig. 2A). Proliferating myoblasts displayed a high resting $[\text{Cl}^-]_i$ of ~82 mM that decreased to ~50 mM within 2.5 h in differentiation medium and remained at 50–60 mM for 48 h (Fig. 2B). Treatment with 100 μM carbenoxolone (CBX), a VRAC inhibitor previously shown to impair myoblast hyperpolarization and differentiation [14], prevented this decrease in $[\text{Cl}^-]_i$ (Fig. 2B), suggesting that VRAC activity accounts for the release of intracellular Cl^- during myogenic commitment.

3.3. A moderate intracellular chloride concentration is required for myoblast fusion

To further explore the role of an intracellular Cl^- decrease during myogenesis, we investigated the effect of Cl^- depletion on myoblast differentiation by assessing the expression of myogenin and myosin, a marker for differentiated cells, in differentiation

medium virtually lacking Cl^- . After 6 h in this medium, C2C12 cells possessed an $[\text{Cl}^-]_i$ of only ~4 mM (Fig. 3A), while $[\text{Cl}^-]_i$ showed the previously observed (Fig. 2B) decrease to ~58 mM in differentiation medium with normal $[\text{Cl}^-]$ (Fig. 3A). However, no difference was observed in either the percentage of myogenin-positive nuclei or total myogenin protein levels between cells with normal or reduced $[\text{Cl}^-]$ during differentiation (Fig. 3B and C). In contrast, myosin expression was significantly inhibited (protein levels in reduced Cl^- were $51 \pm 16\%$ of control, $p = 1.8 \times 10^{-4}$) in Cl^- -reduced medium compared with normal medium (Fig. 3C). We then induced C2C12 cells to differentiate for prolonged periods in either normal or Cl^- -reduced differentiation medium. After 4 days of differentiation, C2C12 myoblasts formed extensive large myotubes in normal medium. In contrast, most myoblasts remained elongated thin cells in Cl^- -reduced medium (Fig. 4A). Immunoblot analysis revealed no difference in the ability of myoblasts to express myogenin in either of the media; however, the expression of myosin was strikingly reduced in Cl^- -reduced medium (Fig. 4B). Notably, this inhibition was not due to the toxicity of low external Cl^- as C2C12 cells were still able to generate large myotubes when the Cl^- -reduced medium was changed to normal medium after two days (Fig. 4A). Hence, a drastic reduction in $[\text{Cl}^-]_i$ does not potentiate myoblast differentiation but may rather impair myoblast fusion.

4. Discussion

Hyperpolarization and an increase in intracellular $[\text{Ca}^{2+}]$ are necessary prerequisites for the terminal differentiation of myoblasts and their fusion into multinucleated myotubes [5–7]. Previously, VRAC was shown to play an important role in skeletal myogenesis by promoting hyperpolarization and the Ca^{2+} signal [14]. However, it remained obscure how VRAC contributes to these processes. VRAC channel activity can lead to osmotic alterations of cell volume and of the membrane potential or conducted osmolytes may function as intra- or extracellular signaling molecules [21]. In addition, physical protein-protein interactions of LRRC8A have

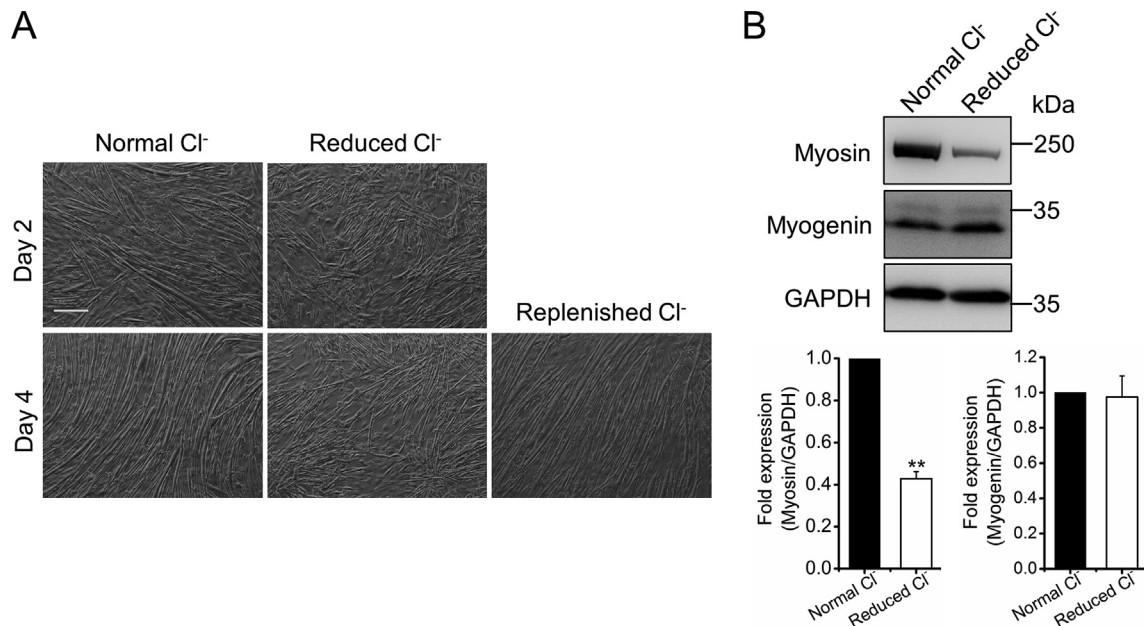


Fig. 4. Reduced extracellular Cl^- impairs myoblast fusion. A, differential interference contrast images of C2C12 cells on the indicated day of differentiation in normal or Cl^- -reduced medium (for 4 days or only for 2 days in the case of washout). Scale bar, 200 μm . B, Immunoblot and quantification of myogenin and myosin protein levels after 4 days of differentiation in normal or Cl^- -reduced medium. Fold changes are relative to normal medium. Data are presented as mean \pm S.D. from three independent experiments. **, $p < 0.01$ using a two-tailed paired t -test.

been proposed to affect intracellular signaling cascades in a conductance-independent manner [15,34]. In this study, we provide twofold evidence for channel activity of VRAC during early C2C12 myoblast differentiation. Firstly, the drop in inter-subunit FRET, which reflects channel opening [24], showed VRAC activity within first 2 h of the differentiation process. The observed temporality of VRAC activity is in agreement with the earlier finding that an inhibition of VRAC starting 6 h after the induction of differentiation did not impinge on this process [14]. Secondly, the observed $[Cl^-]_i$ decrease during the first hours of differentiation was blocked by the VRAC inhibitor CBX, suggesting that the Cl^- efflux is mediated by VRAC. An involvement of VRAC conductance in C2C12 myogenic differentiation is supported by the effect of pharmacological VRAC inhibitors and by the impairment of differentiation by the overexpression of LRRC8A, which suppresses VRAC currents [14,17,18].

We find that proliferating, non-differentiating C2C12 myoblasts possess an unusually high, but not unprecedented [35,36], intracellular Cl^- concentration of ~80 mM. During the sequential hyperpolarization from about -10 mV to about -80 mV that also occurs early in differentiation [9–11], VRAC will mediate Cl^- efflux and result in the observed $[Cl^-]_i$ decrease. Hence, Cl^- conductance by VRAC cannot contribute directly to myoblast hyperpolarization. Instead, hyperpolarization requires the upregulation of Kir2.1 K^+ channels [11]. Their activity is controlled by tyrosine phosphorylation [37]. Changes in intracellular Cl^- may control myogenesis by modulating (de)-phosphorylation events. There are several examples of kinases or phosphatases whose activity is regulated by Cl^- [38]. Cytoplasmic Cl^- has been implicated in further intracellular processes linked to cell differentiation, such as membrane organization [39] and endocytic trafficking [40]. We also find that despite the $[Cl^-]_i$ decrease accompanying myotube formation, an excessive reduction by extracellular Cl^- depletion does not accelerate myoblast differentiation but impairs myoblast fusion. This implies that only a moderate decrease in intracellular Cl^- facilitates this process or that the $[Cl^-]_i$ decrease is not required at all but merely a byproduct of VRAC activity, whose mechanistic involvement in different stages of skeletal myogenesis remains to be explored.

In conclusion, we show the activation of LRRC8-formed volume-regulated anion channels as an early molecular event during myotube formation and a concomitant decrease in intracellular Cl^- . Furthermore, there is a correlation between $[Cl^-]_i$ and myoblast fusion. This report emphasizes the importance of a Cl^- anion and osmolyte channel and provides a new perspective for understanding the signal transduction pathways during skeletal myogenesis.

Declaration of competing interest

The authors declare that they have no conflicts of interests.

Acknowledgments

This work was supported by the German Federal Ministry of Education and Research (BMBF, grant no. 031A314 to T.S.). L.C. holds a fellowship by the Oversea Study Program of Guangzhou Elite Project (No. JY201624). The funders had no role in study design, data collection and analysis, decision to publish, or preparation of the manuscript.

References

- [1] J. Chal, O. Pourqu  , Making muscle: skeletal myogenesis in vivo and in vitro, *Development* 144 (2017) 2104–2122.
- [2] C.F. Bentzinger, Y.X. Wang, M.A. Rudnicki, Building muscle: molecular regulation of myogenesis, *Cold Spring Harb. Perspect. Biol.* 4 (2012) a008342.
- [3] S.M. Hindi, M.M. Tajrishi, A. Kumar, Signaling mechanisms in mammalian myoblast fusion, *Sci. Signal.* 6 (2013) re2.
- [4] P. Bijlenga, J.H. Liu, E. Espinos, C.A. Haenggeli, J. Fischer-Lougheed, C.R. Bader, L. Bernheim, T-type α_1H Ca^{2+} channels are involved in Ca^{2+} signaling during terminal differentiation (fusion) of human myoblasts, *Proc. Natl. Acad. Sci. U.S.A.* 97 (2000) 7627–7632.
- [5] S. Konig, V. Hinard, S. Arnaudeau, N. Holzer, G. Potter, C.R. Bader, L. Bernheim, Membrane hyperpolarization triggers myogenin and myocyte enhancer factor-2 expression during human myoblast differentiation, *J. Biol. Chem.* 279 (2004) 28187–28196.
- [6] S. Arnaudeau, N. Holzer, S. Konig, C.R. Bader, L. Bernheim, Calcium sources used by post-natal human myoblasts during initial differentiation, *J. Cell. Physiol.* 208 (2006) 435–445.
- [7] S. Konig, A. B  quet, C.R. Bader, L. Bernheim, The calcineurin pathway links hyperpolarization (Kir2.1)-induced Ca^{2+} signals to human myoblast differentiation and fusion, *Development* 133 (2006) 3107–3114.
- [8] K. Nakanishi, K. Kakiguchi, S. Yonemura, A. Nakano, N. Morishima, Transient Ca^{2+} depletion from the endoplasmic reticulum is critical for skeletal myoblast differentiation, *Faseb. J.* 29 (2015) 2137–2149.
- [9] P. Bijlenga, T. Occhiodoro, J.H. Liu, C.R. Bader, L. Bernheim, J. Fischer-Lougheed, An ether-  -go K^+ current, I_{h-eag} , contributes to the hyperpolarization of human fusion-competent myoblasts, *J. Physiol.* 512 (Pt 2) (1998) 317–323.
- [10] J.H. Liu, P. Bijlenga, J. Fischer-Lougheed, T. Occhiodoro, A. Kaelin, C.R. Bader, L. Bernheim, Role of an inward rectifier K^+ current and of hyperpolarization in human myoblast fusion, *J. Physiol.* 510 (Pt 2) (1998) 467–476.
- [11] J. Fischer-Lougheed, J.H. Liu, E. Espinos, D. Mordasini, C.R. Bader, D. Belin, L. Bernheim, Human myoblast fusion requires expression of functional inward rectifier Kir2.1 channels, *J. Cell Biol.* 153 (2001) 677–686.
- [12] J.H. Liu, S. K  nig, M. Michel, S. Arnaudeau, J. Fischer-Lougheed, C.R. Bader, L. Bernheim, Acceleration of human myoblast fusion by depolarization: graded Ca^{2+} signals involved, *Development* 130 (2003) 3437–3446.
- [13] G.A. Porter Jr., R.F. Makuck, S.A. Rivkees, Reduction in intracellular calcium levels inhibits myoblast differentiation, *J. Biol. Chem.* 277 (2002) 28942–28947.
- [14] L. Chen, T.M. Becker, U. Koch, T. Stauber, The LRRC8/VRAC anion channel facilitates myogenic differentiation of murine myoblasts by promoting membrane hyperpolarization, *J. Biol. Chem.* 294 (2019) 14279–14288.
- [15] A. Kumar, L. Xie, C.M. Ta, et al., SWELL1-LRRC8 complex regulates skeletal muscle cell size, intracellular signalling, adiposity and glucose metabolism, *BioRxiv* (2020) 2006.2004.134213.
- [16] L. Kumar, J. Chou, C.S. Yee, et al., Leucine-rich repeat containing 8A (LRRC8A) is essential for T lymphocyte development and function, *J. Exp. Med.* 211 (2014) 929–942.
- [17] Z. Qiu, A.E. Dubin, J. Mathur, B. Tu, K. Reddy, L.J. Miraglia, J. Reinhardt, A.P. Orth, A. Patapoutian, SWELL1, a plasma membrane protein, is an essential component of volume-regulated anion channel, *Cell* 157 (2014) 447–458.
- [18] F.K. Voss, F. Ullrich, J. M  nch, K. Lazarow, D. Lutter, N. Mah, M.A. Andrade-Navarro, J.P. von Kries, T. Stauber, T.J. Jentsch, Identification of LRRC8 heteromers as an essential component of the volume-regulated anion channel VRAC, *Science* 344 (2014) 634–638.
- [19] S. Pervaiz, A. Kopp, L. von Kleist, T. Stauber, Absolute protein amounts and relative abundance of volume-regulated anion channel (VRAC) LRRC8 subunits in cells and tissues revealed by quantitative immunoblotting, *Int. J. Mol. Sci.* 20 (2019) 5879.
- [20] B. K  nig, T. Stauber, Biophysics and structure-function relationships of LRRC8-formed volume-regulated anion channels, *Biophys. J.* 116 (2019) 1185–1193.
- [21] L. Chen, B. K  nig, T. Liu, S. Pervaiz, Y.S. Razaque, T. Stauber, More than just a pressure relief valve: physiological roles of volume-regulated LRRC8 anion channels, *Biol. Chem.* 400 (2019) 1481–1496.
- [22] T. Voets, L. Wei, P. De Smet, W. Van Driessche, J. Eggermont, G. Droogmans, B. Nilius, Downregulation of volume-activated Cl^- currents during muscle differentiation, *Am. J. Physiol.* 272 (1997) C667–C674.
- [23] T. Liu, T. Stauber, The volume-regulated anion channel LRRC8/VRAC is dispensable for cell proliferation and migration, *Int. J. Mol. Sci.* 20 (2019) 2663.
- [24] B. K  nig, Y. Hao, S. Schwartz, A.J. Plested, T. Stauber, A FRET sensor of C-terminal movement reveals VRAC activation by plasma membrane DAG signaling rather than ionic strength, *eLife* 8 (2019) e45421.
- [25] B. Pilas, G. Durack, A flow cytometric method for measurement of intracellular chloride concentration in lymphocytes using the halide-specific probe 6-methoxy-N-(3-sulfopropyl) quinolinium (SPQ), *Cytometry* 28 (1997) 316–322.
- [26] J. Schindelin, I. Arganda-Carreras, E. Frise, et al., Fiji: an open-source platform for biological-image analysis, *Nat. Methods* 9 (2012) 676–682.
- [27] J.N. Feige, D. Sage, W. Wahli, B. Desvergne, L. Gelman, PixFRET, an ImageJ plug-in for FRET calculation that can accommodate variations in spectral bleed-throughs, *Microsc. Res. Tech.* 68 (2005) 51–58.
- [28] G. Kasuya, T. Nakane, T. Yokoyama, et al., Cryo-EM structures of the human volume-regulated anion channel LRRC8, *Nat. Struct. Mol. Biol.* 25 (2018) 797–804.
- [29] J.M. Kefauver, K. Saotome, A.E. Dubin, et al., Structure of the human volume regulated anion channel, *eLife* 7 (2018) e38461.
- [30] D. Deneka, M. Sawicka, A.K.M. Lam, C. Paulino, R. Dutzler, Structure of a volume-regulated anion channel of the LRRC8 family, *Nature* 558 (2018)

- 254–259.
- [31] R. Planells-Cases, D. Lutter, C. Guyader, et al., Subunit composition of VRAC channels determines substrate specificity and cellular resistance to Pt-based anti-cancer drugs, *EMBO J.* 34 (2015) 2993–3008.
- [32] D. Lutter, F. Ullrich, J.C. Lueck, S. Kempa, T.J. Jentsch, Selective transport of neurotransmitters and modulators by distinct volume-regulated LRRC8 anion channels, *J. Cell Sci.* 130 (2017) 1122–1133.
- [33] C. Zhou, X. Chen, R. Planells Cases, et al., Transfer of cGAMP into bystander cells via LRRC8 volume-regulated anion channels augments STING-mediated interferon responses and anti-viral immunity, *Immunity* 52 (2020) 767–781, e766.
- [34] Y. Zhang, L. Xie, S.K. Gunasekar, et al., SWELL1 is a regulator of adipocyte size, insulin signalling and glucose homeostasis, *Nat. Cell Biol.* 19 (2017) 504–517.
- [35] H. Kaneko, T. Nakamura, B. Lindemann, Noninvasive measurement of chloride concentration in rat olfactory receptor cells with use of a fluorescent dye, *Am. J. Physiol. Cell Physiol.* 280 (2001) C1387–C1393.
- [36] S. Kim, L. Ma, J. Unruh, S. McKinney, C.R. Yu, Intracellular chloride concentration of the mouse vomeronasal neuron, *BMC Neurosci.* 16 (2015) 90.
- [37] V. Hinard, D. Belin, S. Konig, C.R. Bader, L. Bernheim, Initiation of human myoblast differentiation via dephosphorylation of Kir2.1 K⁺ channels at tyrosine 242, *Development* 135 (2008) 859–867.
- [38] Á.G. Valdivieso, T.A. Santa-Coloma, The chloride anion as a signalling effector, *Biol. Rev. Camb. Philos. Soc.* 94 (2019) 1839–1856.
- [39] M. He, W. Ye, W.J. Wang, E.S. Sison, Y.N. Jan, L.Y. Jan, Cytoplasmic Cl⁻ couples membrane remodeling to epithelial morphogenesis, *Proc. Natl. Acad. Sci. U. S. A.* 114 (2017). E11161–e11169.
- [40] T. Stauber, T.J. Jentsch, Chloride in vesicular trafficking and function, *Annu. Rev. Physiol.* 75 (2013) 453–477.